Hindawi Publishing Corporation
Journal of Nanomaterials
Volume 2015, Article ID 146327, 7 pages
http://dx.doi.org/10.1155/2015/146327

Research Article

Synthesis of Spherical Bi_2WO_6 Nanoparticles by a Hydrothermal Route and Their Photocatalytic Properties

B. Wang, H. Yang, T. Xian, L. J. Di, R. S. Li, and X. X. Wang

School of Science, Lanzhou University of Technology, Lanzhou 730050, China

Correspondence should be addressed to H. Yang; hyang@lut.cn

Received 16 December 2014; Revised 29 January 2015; Accepted 29 January 2015

Academic Editor: Reda Mohamed

Spherical Bi_2WO_6 nanoparticles were synthesized by a hydrothermal route. SEM observation shows that the size of the particles ranges from 60 to 120 nm and the average particle size is ~85 nm. TEM investigation shows that the particles are made up of subgrains with size of 5–10 nm. The bandgap energy of the particles is measured to be 2.93 eV by ultraviolet-visible diffuse reflectance spectroscopy. RhB was chosen as the target pollutant to evaluate the photocatalytic activity of the particles under irradiation of simulated sunlight, revealing that they exhibit an obvious photocatalytic activity. The effects of ethanol, KI, and BQ on the photocatalytic efficiency of Bi_2WO_6 particles towards the RhB degradation were investigated. It is observed that ethanol has no effect on the photocatalytic degradation of RhB, whereas KI and BQ exhibit a substantial suppression of RhB degradation. No hydroxyl (•OH) is found, by the photoluminescence technique using terephthalic acid as a probe molecule, to be produced over the irradiated Bi_2WO_6 particles. Based on the experimental results, photoexcited hole (h^+) and superoxide ($\bullet O_2^-$) are suggested to be the two main active species responsible for the dye degradation, while •OH plays a negligible role in the photocatalysis.

1. Introduction

Environmental pollution and energy shortage are two important global issues that confront mankind today. Semiconductor-based photocatalysis has been attracting great attention due to its promising applications in solving the environmental and energy problems [1, 2]. Aurivillius compounds with general formula $Bi_2A_{n-1}B_nO_{3n+3}$ (A = Ca, Sr, Ba, Pb, Na, K and B = Ti, Nb, Ta, Mo, W, Fe) are known to be an important class of semiconductor oxides. This class of oxides has a special layer structure with perovskite-like units $(A_{n-1}B_nO_{3n+1})^{2-}$ sandwiched between $(Bi_2O_2)^{2+}$ layers and possesses unique physicochemical properties [3]. Bismuth tungstate (Bi_2WO_6) is one of the simplest ($n = 1$) members of the Aurivillius oxides. This oxide exhibits numerous interesting properties such as ferroelectricity, piezoelectricity, nonlinear dielectric susceptibility, gas sensitivity to alcohol, and photocatalytic activity [4–8]. In particular, since Kudo and Hijii found the photocatalytic O_2 evolution from $AgNO_3$ solution over Bi_2WO_6 in 1999 [7] and Tang et al. reported its photocatalytic activity for degrading $CHCl_3$ and CH_3CHO under visible-light irradiation in 2004 [8], Bi_2WO_6 has been extensively studied as a promising visible-light-driven photocatalyst [9–24].

It is known that the photocatalytic activity of a photocatalyst depends on numerous factors, especially the morphology and size. In recent years, various techniques have been widely used to prepare Bi_2WO_6 nano/microcrystals, such as low-temperature combustion method [9], sonochemical approach [10, 11], sol-gel method [12], sol-gel-hydrothermal route [13], coprecipitation method [14], solvothermal method [15], electrospinning technique [16, 17], chemical solution decomposition method [18], ultrasonic-assisted method [19], sucrose templated method [20], and hydrothermal route [21–30]. Among them, the hydrothermal route offers an advantage in controlling the product morphology. Based on the hydrothermal route, several morphologies of Bi_2WO_6 crystals including flower-, nest-, caddice clew-, square plate-, octahedron-, snowflake-, and tyre-like structures have been synthesized [21–30]. In this work, we synthesized for the first time spherical Bi_2WO_6 nanoparticles via a hydrothermal route. The photocatalytic activity of the as-prepared Bi_2WO_6

particles was evaluated by the degradation of rhodamine B (RhB) under simulated-sunlight irradiation. The mechanism involved was systematically investigated and discussed.

2. Experimental

All raw materials and reagents used were of analytical grade without further purification. 0.33 g of $Na_2WO_4{\cdot}2H_2O$ was dissolved in 20 mL distilled water to form solution A, and 0.97 g of $Bi(NO_3)_3{\cdot}5H_2O$ was dissolved in 20 mL acetic acid solution (2.5 mol·L^{-1}) to form solution B. The above process was accompanied by a constant magnetic stirring to make the additives dissolve fully. Then solution A was slowly added to solution B drop by drop under constant magnetic stirring, and immediately a milk-white suspension solution was formed. After being further stirred for 30 min, the suspension solution was adjusted to a pH of 10 by adding NaOH solution (2.5 mol·L^{-1}) and then filled up to 70 mL by adding distilled water. The resultant solution was transferred and sealed in a stainless steel autoclave with a Teflon liner of 100 mL capacity and submitted to hydrothermal treatment at a certain temperature. After a certain time of reaction, the autoclave was naturally cooled down to room temperature. The resultant yellowish precipitate was collected and washed several times with distilled water and absolute ethanol and then dried in a thermostat drying oven at 60°C for 8 h to obtain final Bi_2WO_6 particles.

The phase purity of the as-prepared Bi_2WO_6 particles was examined by means of X-ray powder diffraction (XRD) with Cu Kα radiation. The particle morphology and microstructure were investigated by field-emission scanning electron microscope (SEM) and field-emission transmission electron microscope (TEM). The ultraviolet- (UV-) visible diffuse reflectance spectrum was measured using a UV-visible spectrophotometer equipped with an integrating sphere attachment.

The photocatalytic activity of Bi_2WO_6 particles was evaluated by the degradation of RhB under simulated-sunlight irradiation from a 200 W xenon lamp at room temperature. RhB was dissolved in distilled water to make a 2 mg·L^{-1} RhB solution. The photocatalyst loading was 0.1 g in 100 mL of RhB solution. Before illumination, the mixed solution was mildly stirred by a magnetic bar for 1 h in the dark to reach the adsorption-desorption equilibrium of RhB on the photocatalyst particles. During the photocatalysis experiment, the water-jacketed reactor was cooled with water-cooling system to keep the solution at room temperature. At given irradiation time intervals, a small amount of the reaction solution was sampled for examining the RhB concentration, which was determined by measuring the absorbance of the solution at a fixed wavelength of 554 nm using a UV-visible spectrophotometer. Before the absorbance measurements, the reaction solution was centrifuged at 3000 r·min^{-1} for 10 min to remove the photocatalyst. The effects of ethanol, KI, and benzoquinone (BQ) on the photocatalytic efficiency were investigated, aiming at revealing the dominant species responsible for the dye degradation.

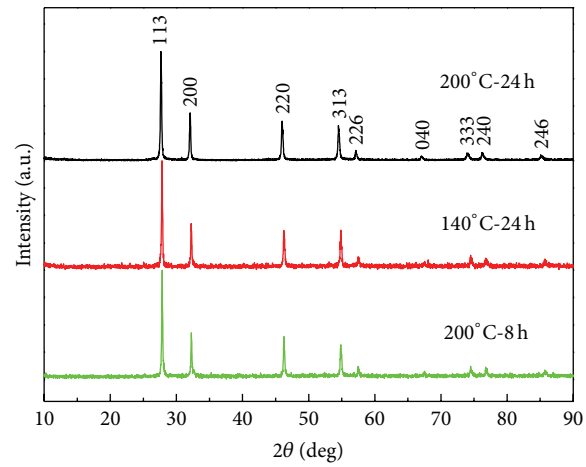

Figure 1: XRD patterns of Bi_2WO_6 particles prepared at different hydrothermal reaction temperatures and times.

A photoluminescence (PL) technique was used to examine the hydroxyl (•OH) radicals formed over the irradiated Bi_2WO_6 as well as P25 photocatalysts by using terephthalic acid (TPA) as a probe molecule. TPA tends to react with •OH radicals to produce 2-hydroxyterephthalic acid (TAOH) that is a highly fluorescent compound. The PL intensity of TAOH at around 429 nm is in proportion to the amount of produced •OH radicals. TPA was dissolved in sodium hydroxide solution (1.0 mmol·L^{-1}) to make a 0.25 mmol·L^{-1} TPA solution. 0.1 g of the photocatalyst was added to 100 mL of the TPA solution. After being magnetically stirred for several minutes in the dark, the mixed solution was irradiated by a 200 W xenon lamp (simulated sunlight). The reaction solution was centrifuged at 3000 r·min^{-1} for 10 min to remove the photocatalyst. The upper clear solution in the centrifuge tube was used for the PL measurements at a fluorescence spectrophotometer with the excitation wavelength of 315 nm.

3. Results and Discussion

Figure 1 shows the XRD patterns of Bi_2WO_6 particles prepared at different hydrothermal reaction temperatures and times (the samples are separately denoted as 200°C-24 h, 140°C-24 h, and 200°C-8 h). It is seen that all the diffraction peaks of Bi_2WO_6 particles can be indexed in terms of the orthorhombic Bi_2WO_6 phase (PDF card number 73-2020), and no traces of other impurity phases are detected in the XRD patterns.

Figures 2(a)–2(c) show the SEM images of 200°C-24 h, 140°C-24 h, and 200°C-8 h samples, respectively, revealing that the particles are regularly shaped like spheres without any adhesive behavior. For all the samples, the size of the particles ranges from 60 to 120 nm and the average particle size is ~85 nm. This indicates that the hydrothermal reaction temperature and time have almost no effect on the particle size.

Figure 3(a) shows the TEM image of 200°C-24 h sample, revealing a spherical morphology with an average particle size of ~85 nm, which is well in agreement with the SEM

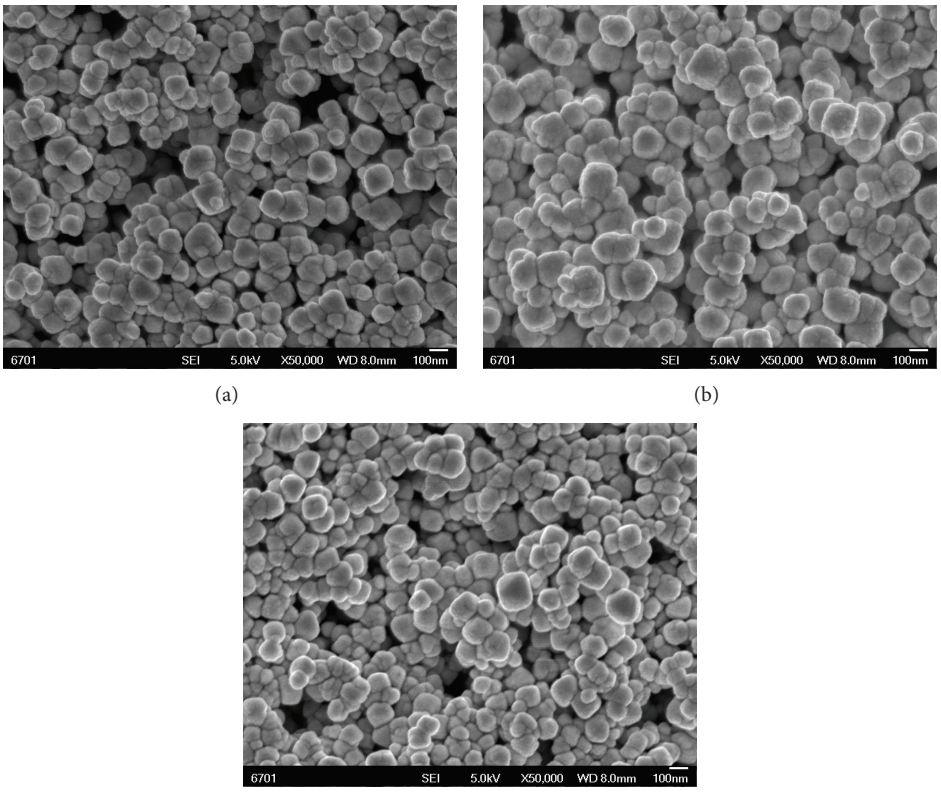

(a) (b)

(c)

Figure 2: SEM images of Bi_2WO_6 particles. (a) 200°C-24 h, (b) 140°C-24 h, and (c) 200°C-8 h.

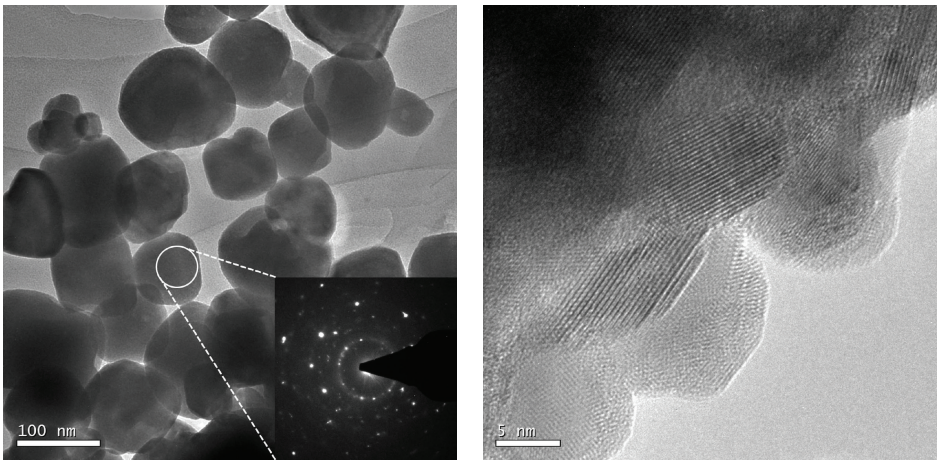

(a) (b)

Figure 3: (a) TEM image of Bi_2WO_6 particles (200°C-24 h sample). The insert shows the SAED pattern of a single particle. (b) High-resolution TEM image obtained from a particle.

observation. The selected area electron diffraction (SAED) pattern of a single particle is inserted in Figure 3(a), which presents clearly polycrystalline diffraction rings. This indicates that the individual particle is not a single crystal but is composed of several grains or subgrains. Figure 3(b) gives the high-resolution TEM image obtained from a particle, showing that the particle is made up of subgrains with size of 5–10 nm.

Figure 4 shows the UV-visible diffuse reflectance spectra of Bi_2WO_6 samples. The insert in Figure 4 shows the corresponding first derivative of the reflectance (R) with respect to wavelength λ (i.e., $dR/d\lambda$). The absorption edge ascribable to

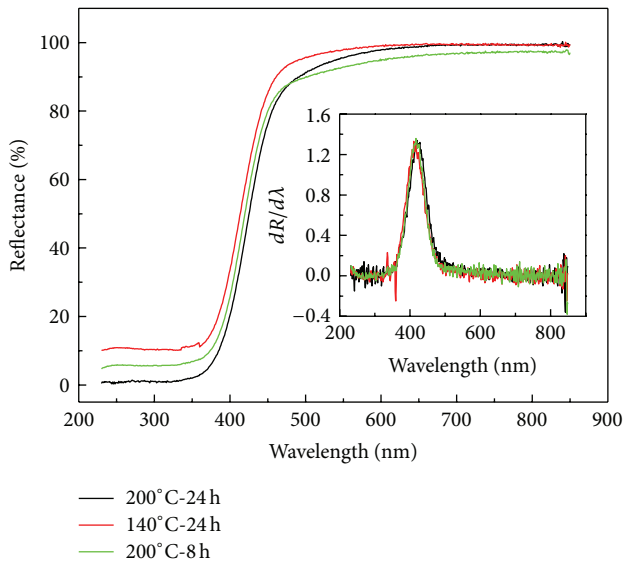

FIGURE 4: UV-visible diffuse reflectance spectra of Bi_2WO_6 samples. The insert shows the corresponding first derivative of the diffuse reflectance spectra.

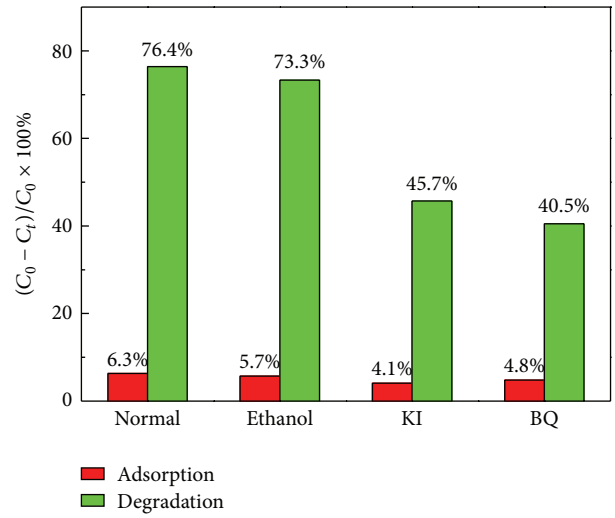

FIGURE 6: Effects of ethanol (5% by volume), KI (1.0 mmol·L^{-1}), and BQ (1.0 mmol·L^{-1}) on the photocatalytic degradation rate of RhB at a testing of 5 h (where 200°C-24 h sample is used as the photocatalyst), along with the corresponding adsorption rates after 1 h in the dark.

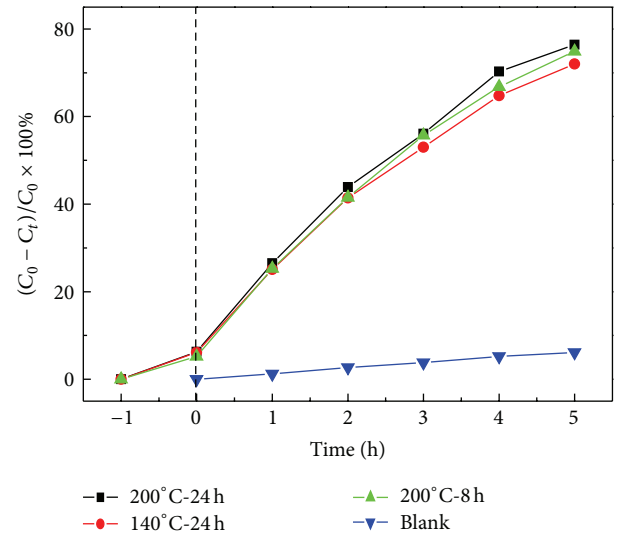

FIGURE 5: Photocatalytic degradation of RhB over Bi_2WO_6 samples as a function of irradiation time, along with the blank experiment results.

the electron transition from valence band to conduction band can be determined from the peak wavelength in the first derivative spectra. All the samples have a similar absorption edge located at 423 nm, from which the bandgap energy E_g of the samples is obtained to be 2.93 eV.

Figure 5 shows the photocatalytic degradation of RhB over Bi_2WO_6 samples as a function of irradiation time (t), along with the blank experiment results. C_0 is the initial concentration of RhB and C_t is the RhB concentration after irradiation for time t. In the absence of the photocatalyst, RhB appears to be stable under simulated-sunlight irradiation and its degradation percentage is only ~6.1% after 5 h of exposure.

In the absence of simulated-sunlight irradiation, Bi_2WO_6 samples show a moderate adsorption toward RhB (about 5.2–6.3% after 1 h of adsorption). On irradiation with simulated sunlight in the presence of Bi_2WO_6 samples, the degradation of RhB increases substantially with increasing irradiation time and reaches ~76.4, ~72, and ~74.9% after 5 h of irradiation for 200°C-24 h, 140°C-24 h, and 200°C-8 h samples, respectively. These values are much larger than the blank degradation as well as the adsorption value, implying a pronounced photocatalytic activity of as-prepared Bi_2WO_6 particles toward the dye degradation.

It is known that ethanol and BQ can be, respectively, used as the scavenger of •OH and superoxide ($\bullet O_2^-$), whereas KI is an efficient scavenger to both •OH and photoexcited h^+ [31, 32]. By investigating the effects of ethanol, KI, and BQ on the photocatalytic efficiency of Bi_2WO_6 particles toward the RhB degradation, we can clarify the role of •OH, h^+, and $\bullet O_2^-$ in the photocatalysis. Figure 6 shows the effects of ethanol (5% by volume), KI (1.0 mmol·L^{-1}), and BQ (1.0 mmol·L^{-1}) on the photocatalytic degradation rate of RhB at testing of 5 h, where 200°C-24 h sample is used as the photocatalyst. The corresponding adsorption rate after 1 h in the dark is also given in Figure 6, which demonstrates a minor change when adding the scavengers. The photocatalytic results show that ethanol has almost no effect on the photocatalytic degradation of RhB. This indicates a negligible role of •OH in the dye degradation. However, KI and BQ exhibit a substantial suppression of RhB degradation, which implies that h^+ and $\bullet O_2^-$ are the dominant active species responsible for the dye degradation over Bi_2WO_6 particles.

Figure 7 shows the PL spectra of the TPA solution after reaction for 3 h over the simulated-sunlight irradiated Bi_2WO_6 (200°C-24 h sample) and P25 photocatalysts. It is well known that •OH radicals can be readily generated over the irradiated commercial Degussa P25 (a mixed-phase TiO_2

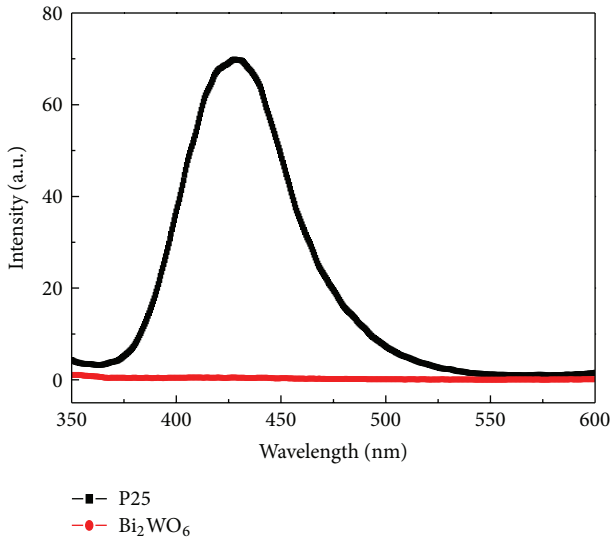

FIGURE 7: PL spectra of the TPA solution after reaction for 3 h over the simulated-sunlight irradiated Bi_2WO_6 (200°C-24 h sample) and P25 photocatalysts.

photocatalyst) in water solution [33]. As a result, when P25 is used as a photocatalyst, the TPA reaction solution shows obvious PL signal at around 429 nm. However, on irradiation in the presence of Bi_2WO_6 photocatalyst, the TPA reaction solution shows no PL signal at around 429 nm, indicating no •OH radicals produced over the irradiated Bi_2WO_6 photocatalyst. This result further reveals that •OH radicals play a minor or negligible role in the dye degradation.

Generally, the conduction band (CB) and valence band (VB) edge potentials of a semiconductor play a key role in the photocatalysis process. In Bi_2WO_6, the hybridized O 2p and Bi 6s states form the top of valence band while the W 5d states form the bottom of conduction band, where the energy difference between the valence and conduction bands is known as the forbidden energy gap (E_g) [34]. The conduction band and valence band potentials of Bi_2WO_6 can be calculated using the following relation [35]:

$$E_{CB} = X - E^e - 0.5E_g \qquad \left(\text{or } E_{VB} = X - E^e + 0.5E_g\right), \tag{1}$$

where X is the absolute electronegativity of Bi_2WO_6 (defined as the arithmetic mean of the electron affinity and the first ionization of the constituent atoms) and is estimated to be 6.2 eV according to the data reported in the literature [36], E^e is the energy of free electrons on the hydrogen scale (4.5 eV), and E_g is the bandgap energy of Bi_2WO_6 (2.93 eV). The conduction band and valence band potentials of Bi_2WO_6 particles versus normal hydrogen electrode (NHE) are therefore calculated to be +0.24 and +3.17 V, respectively.

When Bi_2WO_6 is irradiated with light of energy greater than its E_g, electrons are excited from the valence band to the conduction band, thus generating e^-/h^+ pairs. The photoexcited electrons and holes migrate to the Bi_2WO_6 particle surface and participate in a series of redox reactions to produce a number of active species. Generally, $\bullet O_2^-$ that is suggested to be a dominant active species in the photocatalysis is derived from the reaction of the photoexcited e^- and O_2. From a thermodynamic point of view, the conduction band potential of a semiconductor is required to be negative to the redox potential of $O_2/\bullet O_2^-$ (−0.13 V versus NHE [37]) so that the reaction between e^- and O_2 can proceed. Although the conduction band potential of Bi_2WO_6 particles calculated from (1) is positive to the redox potential of $O_2/\bullet O_2^-$, their actual value in the solution could be changed. It is noted that the conduction band potential of a semiconductor has an increasing trend with the solution pH [38]. In our photocatalytic experiments, the pH value of the reaction solution is measured to be 6.5, which is much higher than (pH = 0) when calculating the conduction band potential. This indicates that the conduction band potential of Bi_2WO_6 particles in the solution is expected to undergo a negative shift compared to their calculated value, consequently making the generation of $\bullet O_2^-$ from the reaction between e^- and O_2 thermodynamically possible.

The redox potentials of $OH^-/\bullet OH$ and $H_2O/\bullet OH$ are +1.89 and +2.72 V versus NHE [39], respectively, both of which are negative to the valence band potential of Bi_2WO_6 (+3.17 V). From this point of view, it seems that the photoexcited h^+ can readily react with OH^- and H_2O to produce •OH radicals. However, no •OH is found to be produced over the irradiated Bi_2WO_6 particles. A possible reason is that the photoexcited h^+ forms as Bi^{5+} oxidation state, and the redox potential of Bi^{5+}/Bi^{3+}, being +1.59 V versus NHE [40], is negative to those of $OH^-/\bullet OH$ and $H_2O/\bullet OH$. This makes it reasonable that the photoexcited h^+ cannot react with OH^-/H_2O to generate •OH.

The reusability of Bi_2WO_6 particles was examined by the recycling photocatalytic experiment. After the first cycle of the photocatalysis was completed, the catalyst was collected by centrifugation, washed with water, and dried. The recovered catalyst was introduced to the fresh RhB solution for the next cycle of the photocatalytic experiment under the same conditions. This process was repeated four times. Figure 8 shows the degradation of RhB after simulated-sunlight irradiation for 5 h over Bi_2WO_6 particles (200°C-24 h sample) during the five photocatalytic cycles. It reveals that the degradation percentage of RhB maintains 75% to 76% for five consecutive recycles. This indicates an excellent photocatalytic reusability of Bi_2WO_6 particles.

4. Conclusion

Spherical Bi_2WO_6 nanoparticles with an average size of ~85 nm were synthesized by a hydrothermal route. The individual particle is made up of subgrains with size of 5–10 nm. The bandgap energy of the particles is obtained to be 2.93 eV. The photocatalytic activity of the particles was evaluated by degrading RhB under simulated-sunlight irradiation, and the effects of ethanol, KI, and BQ on the photocatalytic efficiency were investigated. The results reveal that the photocatalytic degradation of RhB has no dependence on ethanol but is substantially suppressed by the addition of KI and BQ. No

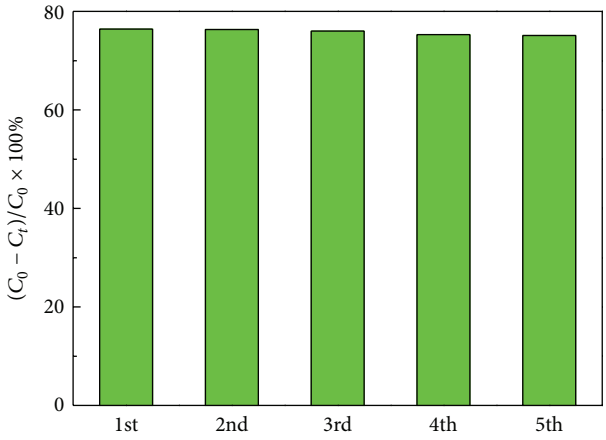

Figure 8: Degradation of RhB after simulated-sunlight irradiation for 5 h over Bi_2WO_6 particles during five photocatalytic cycles.

•OH is found to be produced over the irradiated Bi_2WO_6 particles. Based on the experimental results, we suggest that h^+ and $\bullet O_2^-$ are the dominant active species causing the dye degradation, while •OH plays a negligible role in the photocatalysis. In addition, Bi_2WO_6 particles exhibit good stability in their photocatalytic activity according to recycling photocatalytic experiments.

Conflict of Interests

The authors declare that there is no conflict of interests regarding the publication of this paper.

Acknowledgments

This work was supported by the National Natural Science Foundation of China (Grant no. 51262018), the Fundamental Research Funds for Universities of Gansu Province (Grant no. 056003), and the Hongliu Outstanding Talents Foundation of Lanzhou University of Technology (Grant no. J201205).

References

[1] A. Mills, R. H. Davies, and D. Worsley, "Water purification by semiconductor photocatalysis," *Chemical Society Reviews*, vol. 22, no. 6, pp. 417–425, 1993.

[2] M. R. Hoffmann, S. T. Martin, W. Choi, and D. W. Bahnemann, "Environmental applications of semiconductor photocatalysis," *Chemical Reviews*, vol. 95, no. 1, pp. 69–96, 1995.

[3] B. Frit and J. P. Mercurio, "The crystal chemistry and dielectric properties of the Aurivillius family of complex bismuth oxides with perovskite-like layered structures," *Journal of Alloys and Compounds*, vol. 188, pp. 27–35, 1992.

[4] H. W. Newkirk, P. Quadflieg, J. Liebertz, and A. Kockel, "Growth, crystallography and dielectric properties of Bi2WO6," *Ferroelectrics*, vol. 4, no. 1, pp. 51–55, 1972.

[5] V. I. Utkin, Y. E. Roginskaya, V. I. Voronkova, V. K. Yanovskii, B. S. Galyamov, and Y. N. Ventevtsev, "Dielectric properties, electrical conductivity, and relaxation phenomena in ferroelectric Bi_2WO_6," *Physica Status Solidi A*, vol. 59, no. 1, pp. 75–82, 1980.

[6] D. J. Wang, G. L. Xue, Y. Z. Zhen, F. Fu, and D. S. Li, "Monodispersed Ag nanoparticles loaded on the surface of spherical Bi_2WO_6 nanoarchitectures with enhanced photocatalytic activities," *Journal of Materials Chemistry*, vol. 22, no. 11, pp. 4751–4758, 2012.

[7] A. Kudo and S. Hijii, "H_2 or O_2 evolution from aqueous solutions on layered oxide photocatalysts consisting of Bi^{3+} with $6s^2$ configuration and d^0 transition metal ions," *Chemistry Letters*, no. 10, pp. 1103–1104, 1999.

[8] J. W. Tang, Z. J. Zou, and J. H. Ye, "Photocatalytic decomposition of organic contaminants by Bi_2WO_6 under visible light irradiation," *Catalysis Letters*, vol. 92, no. 1-2, pp. 53–56, 2004.

[9] Z. J. Zhang, W. Z. Wang, M. Shang, and W. Z. Yin, "Low-temperature combustion synthesis of Bi_2WO_6 nanoparticles as a visible-light-driven photocatalyst," *Journal of Hazardous Materials*, vol. 177, no. 1–3, pp. 1013–1018, 2010.

[10] F.-J. Zhang, F.-Z. Xie, J. Liu, W. Zhao, and K. Zhang, "Rapid sonochemical synthesis of irregular nanolaminar-like Bi_2WO_6 as efficient visible-light-active photocatalysts," *Ultrasonics Sonochemistry*, vol. 20, no. 1, pp. 209–215, 2013.

[11] V. D. Nithya, R. K. Selvan, D. Kalpan, L. Vasylechko, and C. Sanjeeviraj, "Synthesis of Bi_2WO_6 nanoparticles and its electrochemical propertiesin different electrolytes for pseudocapacitor electrodes," *Electrochimica Acta*, vol. 109, pp. 720–731, 2013.

[12] G. K. Zhang, F. Lu, M. Li, J. L. Yang, X. Y. Zhang, and B. B. Huang, "Synthesis of nanometer Bi_2WO_6 synthesized by sol–gel method and its visible-light photocatalytic activity for degradation of 4BS," *Journal of Physics and Chemistry of Solids*, vol. 71, no. 4, pp. 579–582, 2010.

[13] Y. M. Li, Z. J. Li, H. Lv, H. B. Tang, and X. Y. Xing, "Synthesis of hierarchical Bi_2WO_6 microspheres with high visible-light-driven photocatalytic activities by sol–gel-hydrothermal route," *Materials Letters*, vol. 108, pp. 84–87, 2013.

[14] S. O. Alfaro and A. M. D. Cruz, "Synthesis, characterization and visible-light photocatalytic properties of Bi_2WO_6 and $Bi_2W_2O_9$ obtained by co-precipitation method," *Applied Catalysis A: General*, vol. 383, no. 1-2, pp. 128–133, 2010.

[15] Y. W. Mi, S. Y. Zeng, L. Li et al., "Solvent directed fabrication of Bi_2WO_6 nanostructures with different morphologies: synthesis and their shape-dependent photocatalytic properties," *Materials Research Bulletin*, vol. 47, no. 9, pp. 2623–2630, 2012.

[16] M. Shang, W. Wang, J. Ren, S. Sun, L. Wang, and L. Zhang, "A practical visible-light-driven Bi_2WO_6 nanofibrous mat prepared by electrospinning," *Journal of Materials Chemistry*, vol. 19, no. 34, pp. 6213–6218, 2009.

[17] G. Zhao, S. Liu, and Q. F. Lu, "One-dimensional Bi_2WO_6 nanofibers controllable synthesis by electrospinning and enhanced visible photocatalytic degradation performances," *Journal of Cluster Science*, vol. 24, no. 2, pp. 523–530, 2013.

[18] G. Q. Zhang, N. Chang, D. Q. Han, A. Q. Zhou, and X. H. Xu, "The enhanced visible light photocatalytic activity of nanosheet-like Bi_2WO_6 obtained by acid treatment for the degradation of rhodamine B," *Materials Letters*, vol. 64, no. 19, pp. 2135–2137, 2010.

[19] L. Zhou, W. Z. Wang, and L. S. Zhang, "Ultrasonic-assisted synthesis of visible-light-induced Bi_2MO_6 (M = W, Mo) photocatalysts," *Journal of Molecular Catalysis A: Chemical*, vol. 268, no. 1-2, pp. 195–200, 2007.

[20] S. M. M Zawawi, R. Yahya, A. Hassan, H. N. M. E. Mahmud, and M. N. Daud, "Structural and optical characterization of metal

tungstates (MWO4; M=Ni, Ba, Bi) synthesized by a sucrose-templated method," *Chemistry Central Journal*, vol. 7, no. 1, article 80, 2013.

[21] Y. Tian, G. M. Hua, W. Xu, N. Li, M. Fang, and L. D. Zhang, "Bismuth tungstate nano/microstructures: controllable morphologies, growth mechanism and photocatalytic properties," *Journal of Alloys and Compounds*, vol. 509, no. 3, pp. 724–730, 2011.

[22] H. Wang, J. M. Song, H. Zhang, F. Gao, S. J. Zhao, and H. Q. Hu, "Controlled synthesis of three-dimensional hierarchical Bi_2WO_6 microspheres with optimum photocatalytic activity," *Materials Research Bulletin*, vol. 47, no. 2, pp. 315–320, 2012.

[23] P. Dumrongrojthanath, T. Thongtem, A. Phuruangrat, and S. Thongtem, "Hydrothermal synthesis of Bi_2WO_6 hierarchical flowers with their photonic and photocatalytic properties," *Superlattices and Microstructures*, vol. 54, no. 1, pp. 71–77, 2013.

[24] J. Y. He, W. M. Wang, F. Long, Z. G. Zou, Z. Y. Fu, and Z. Xu, "Hydrothermal synthesis of hierarchical rose-like Bi_2WO_6 microspheres with high photocatalytic activities under visible-light irradiation," *Materials Science and Engineering: B*, vol. 177, no. 12, pp. 967–974, 2012.

[25] Y. Q. Zhuo, J. F. Huang, L. Y. Cao, H. B. Ouyang, and J. P. Wu, "Photocatalytic activity of snow-like Bi_2WO_6 microcrystalline for decomposition of Rhodamine B under natural sunlight irradiation," *Materials Letters*, vol. 90, pp. 107–110, 2013.

[26] W. L. Lee, S. T. Huang, J. L. Chang, J. Y. Chen, C. M. Cheng, and C. C. Chen, "Photodegradation of CV over nanocrystalline bismuth tungstate prepared by hydrothermal synthesis," *Journal of Molecular Catalysis A: Chemical*, vol. 361–362, pp. 80–90, 2012.

[27] Y. H. B. Liao, J. X. Wang, J. S. Lin, W. H. Chung, W. Y. Lin, and C. C. Chen, "Synthesis, photocatalytic activities and degradation mechanism of Bi_2WO_6 toward crystal violet dye," *Catal Today*, vol. 174, no. 1, pp. 148–159, 2011.

[28] L. An, G. H. Wang, X. Zhou, Y. Wang, F. Gao, and Y. Cheng, "Preparation of Ag-loaded octahedral Bi_2WO_6 photocatalyst and its photocatalytic activity," *Russian Journal of Physical Chemistry A*, vol. 88, no. 13, pp. 2424–2428, 2014.

[29] R. M. Mohamed and E. S. Aazam, "Enhancement of photocatalytic properties of Bi_2WO_6 nanoparticles by Pt deposition," *Materials Research Bulletin*, vol. 48, no. 9, pp. 3572–3578, 2013.

[30] X. Lin, Z. X. Liu, X. Y. Guo et al., "Controllable synthesis and photocatalytic activity of spherical, flower-like and nanofibrous bismuth tungstates," *Materials Science and Engineering: B*, vol. 188, pp. 35–42, 2014.

[31] T. Xian, H. Yang, W. Xian, X. F. Chen, and J. F. Dai, "Photocatalytic mechanism of $Bi_2Fe_4O_9$ nanoparticles in the degradation of methylene blue," *Progress in Reaction Kinetics and Mechanism*, vol. 38, no. 4, pp. 417–424, 2013.

[32] W. Liu, M. L. Wang, C. X. Xu, and S. F. Chen, "Facile synthesis of g-C_3N_4/ZnO composite with enhanced visible light photooxidation and photoreduction properties," *Chemical Engineering Journal*, vol. 209, pp. 386–393, 2012.

[33] H. Czili and A. Horvath, "Applicability of coumarin for detecting and measuring hydroxyl radicals generated by photoexcitation of TiO_2 nanoparticles," *Applied Catalysis B: Environmental*, vol. 81, no. 3-4, pp. 295–302, 2008.

[34] H. B. Fu, L. W. Zhang, W. Q. Yao, and Y. F. Zhu, "Photocatalytic properties of nanosized Bi_2WO_6 catalysts synthesized via a hydrothermal process," *Applied Catalysis B: Environmental*, vol. 66, no. 1-2, pp. 100–110, 2006.

[35] S. R. Morrison, *Electrochemistry at Semiconductor and Oxidized Metal Electrodes*, Plenum Press, New York, NY, USA, 1980.

[36] T. Andersen, H. K. Haugen, and H. Hotop, "Binding energies in atomic negative ions: III," *Journal of Physical and Chemical Reference Data*, vol. 28, no. 6, pp. 1511–1533, 1999.

[37] T. Arai, M. Yanagida, Y. Konishi, Y. Lwasaki, H. Sugihara, and K. Sayama, "Efficient complete oxidation of acetaldehyde into CO_2 over $CuBi_2O_4/WO_3$ composite photocatalyst under visible and UV light irradiation," *The Journal of Physical Chemistry C*, vol. 111, no. 21, pp. 7574–7577, 2007.

[38] D. Dung, J. Ramsden, and M. Gratzel, "Dynamics of interfacial electron-transfer processes in colloidal semiconductor systems," *Journal of the American Chemical Society*, vol. 104, no. 11, pp. 2977–2985, 1982.

[39] T. Tachikawa, M. Fujitsuka, and T. Majima, "Mechanistic insight into the TiO_2 photocatalytic reactions: design of new photocatalysts," *The Journal of Physical Chemistry C*, vol. 111, no. 14, pp. 5259–5275, 2007.

[40] R. C. Weast, *Handbook of Chemistry and Physics*, CRC Press, Boca Raton, Fla, USA, 1988.